Medical Physics
The International Journal of Medical Physics Research and Practice

# Three-dimensional ultrasound system for guided breast brachytherapy

Paul De Jean, Luc Beaulieu, and Aaron Fenster

Citation: Medical Physics **36**, 5099 (2009); doi: 10.1118/1.3243865
View online: http://dx.doi.org/10.1118/1.3243865
View Table of Contents: http://scitation.aip.org/content/aapm/journal/medphys/36/11?ver=pdfcov
Published by the American Association of Physicists in Medicine



# Three-dimensional ultrasound system for guided breast brachytherapy

Paul De Jean[a)]
*Imaging Research Laboratories, Robarts Research Institute, The University of Western Ontario, London, Ontario N6A 5K8, Canada and Department of Medical Biophysics, The University of Western Ontario, London, Ontario N6A 5C1, Canada*

Luc Beaulieu
*Département de Radio-oncologie et Centre de recherche en Cancérologie de l'Université Laval, Centre Hospitalier Universitaire de Québec, Québec, Québec G1R 2J6, Canada and Département de Physique, de Génie Physique et d'Optique, Université Laval, Québec, Québec G1R 2J6, Canada*

Aaron Fenster
*Imaging Research Laboratories, Robarts Research Institute, The University of Western Ontario, London, Ontario N6A 5K8, Canada, Department of Medical Biophysics, The University of Western Ontario, London, Ontario N6A 5C1, Canada and Biomedical Engineering Graduate Program, The University of Western Ontario, London, Ontario N6A 5B9, Canada*

(Received 13 January 2009; revised 14 September 2009; accepted for publication 16 September 2009; published 8 October 2009)

Breast-conserving surgery combined with subsequent radiation therapy is a standard procedure in breast cancer treatment. The disadvantage of whole-breast beam irradiation is that it requires 20–25 treatment days, which is inconvenient for patients with limited mobility or who reside far from the treatment center. However, interstitial high-dose-rate (HDR) brachytherapy is an irradiation method requiring only 5 treatment days and that delivers a lower radiation dose to the surrounding healthy tissue. It involves delivering radiation through $^{192}$Ir seeds placed inside the catheters, which are inserted into the breast. The catheters are attached to a HDR afterloader, which controls the seed placement within the catheters and irradiation times to deliver the proper radiation dose. One disadvantage of using HDR brachytherapy is that it requires performing at least one CT scan during treatment planning. The procedure at our institution involves the use of two CT scans. Performing CT scans requires moving the patient from the brachytherapy suite with catheters inserted in their breasts. One alternative is using three-dimensional ultrasound (3DUS) to image the patient. In this study, the authors developed a 3DUS translation scanning system for use in breast brachytherapy. The new system was validated using CT, the current clinical standard, to image catheters in a breast phantom. Once the CT and 3DUS images were registered, the catheter trajectories were then compared. The results showed that the average angular separation between catheter trajectories was 2.4°, the average maximum trajectory separation was 1.0 mm, and the average mean trajectory separation was found to be 0.7 mm. In this article, the authors present the 3DUS translation scanning system's capabilities as well as its potential to be used as the primary treatment planning imaging modality in breast brachytherapy. © *2009 American Association of Physicists in Medicine*. [DOI: 10.1118/1.3243865]

Key words: breast cancer, 3D ultrasound, image guidance, brachytherapy

## I. INTRODUCTION

### I.A. Background on breast radiotherapy

Breast-conserving surgery or lumpectomy, followed by radiation therapy, is becoming an increasingly common form of treatment for patients with smaller breast tumors as it has a similar success rate as a full radical mastectomy and minimizes breast disfigurement.[1,2] One method commonly used to deliver radiation is whole-breast external beam radiotherapy. This involves the delivery of 45–50 Gy of radiation dose to the entire breast over 20–25 fractions, spanning 5 to 7 weeks.[3,4] Patients with limited mobility or who reside a great distance away from the treatment location are greatly inconvenienced by the length of this treatment. Thus, current research is focused on developing methods that reduce the number of treatment days. One such method is partial breast irradiation, an alternative form of treatment that enables the delivery of radiation dose to only a prescribed tumor margin. The advantage of partial breast irradiation is twofold: Not only does it potentially reduce the dose delivered to the surrounding healthy tissues, it also greatly reduces the length of the treatment. While it may seem counterintuitive to reduce radiation coverage in the hopes of enhancing tumor elimination, studies have shown that most failures occur at the site of the primary resected lesion.[5,6] Partial breast irradiation delivery can be achieved through three-dimensional (3D) external radiotherapy, MammoSite brachytherapy, or interstitial brachytherapy. Treatment time for all of these procedures is only 4–5 days,[3,7] and patients are treated on an outpatient basis.

Partial breast irradiation through external beam radiation therapy or radiosurgery delivers radiation dose only to a specific region near the tumor bed. This procedure uses a linear accelerator or $^{60}$Co radiation therapy delivery system. While treatment planning for this procedure is more involved than for standard external beam radiotherapy, it results in shorter treatment periods and a reduced dose to the surrounding healthy tissue.[8,9]

Mammosite brachytherapy (Hologic, Inc., Bedford, MA) involves the insertion of a mammosite balloon catheter within the tumor cavity.[10] The balloon at the end of this catheter is first filled with saline. Next, the balloon is attached to a high-dose-rate (HDR) afterloader, which places an $^{192}$Ir seed at the center of the saline balloon.[10]

HDR interstitial brachytherapy involves the delivery of radiation to specific regions by inserting radioactive $^{192}$Ir seeds into catheters, which are placed inside the breast. The dwell positions of the source within the catheters and irradiation time (dwell time) are controlled using a HDR afterloader, which is attached to the interstitial catheters during treatment. The results from studies performing partial breast irradiation using interstitial brachytherapy on stage I or II breast cancer are encouraging: Local control rates have varied between 91.2% and 100%,[7,11–16] while cosmetic results have been either good or excellent in 67%–100% of previous studies.[7,11–16]

When delivering radiation dose using interstitial brachytherapy, computed tomography (CT) is the current imaging standard for treatment planning. In our collaborating institution at Université Laval in Quebec City, two CT scans are required to complete treatment planning. The first is a preplanning scan obtained with a brachytherapy template in place. The CT scan is used to delineate tumor margins and determine which catheters need to be inserted into the breast to deliver the final brachytherapy treatment. The second CT scan is used to plan radiation delivery with all interstitial catheters in place. One drawback of using CT is that it requires the patient to be moved from the brachytherapy suite to a CT suite to be imaged. This displacement can cause the patient a great deal of discomfort, as the catheters must remain inserted in the patient's breast throughout the entire process. Due to the fact that performing CT scans involves moving the patient, it requires a great deal of time and manpower, increasing the cost of the procedure. Moving the patient from the CT suite to the brachytherapy suite following the preplanning scan can also result in slight changes in the tumor geometry relative to the template. Another disadvantage of performing a CT scan is that it images an entire region of the patient's torso, subjecting the patient's surrounding healthy tissue to an additional radiation dose.

Alternatively, some institutions determine the approximate location of the tumor bed using freehand 2DUS. While this procedure saves time overall, it also results in more catheters than necessary being inserted into the breast to deliver the radiation dose, thus resulting in more puncture scars on the patient's breast. The increase in the number of inserted catheters is a result of wanting to cover the entire tumor cavity area while not having an image that displays the relative cavity geometry in three dimensions. Additionally, this procedure is complicated by the physical difficulty in simultaneously controlling the US probe while inserting the needle into the breast.

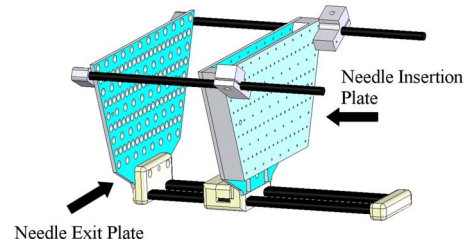


FIG. 1. The Kuske breast applicator set. The patient's breast is placed in between the two plates of the template. The plates compress the breast, and brachytherapy needles are fed through the holes on each side of the template. The needle insertion and exit plates are indicated on the figure.

In order to avoid moving the patient while still keeping the number of inserted catheters to a minimum, we propose using a three-dimensional ultrasound (3DUS) as the alternative imaging modality for intraprocedural treatment planning. We have designed a system that incorporates 3DUS imaging into existing HDR brachytherapy protocol. In this study, we describe the 3DUS translation scanner design and examine its ability to image catheter locations in phantoms. A standard treatment plan is used and 3DUS images are compared to an image produced by a CT scanner.

### I.B. HDR breast brachytherapy procedure already in place

Following their surgery, eligible patients undergo partial breast irradiation. The existing breast brachytherapy protocol involves the insertion of catheters into the breast in locations either through or near the resected tumor cavity. Regions within 1.5 cm outside the tumor cavity are regarded as targeting tissues. The postsurgical fluid-filled cavity is located with a 2DUS using a US machine (B-K Falcon 2101, B-K Medical, Herlev, Denmark) coupled to a US probe (B-K 8811, B-K Medical, Herlev, Denmark). In order to ensure the catheters are placed so as to effectively deliver radiation dose, we guide the inserted catheters using a breast brachytherapy template (Kuske breast applicator set, Nucletron, Veenendaal, The Netherlands), as shown in Fig. 1. The template consists of parallel trapezoid-shaped plates composed of a special plastic with proprietary composition connected by carbon rods. The plates are moved along the rods and then locked in position, compressing the breast sufficiently so that it cannot shift during the needle insertion procedure. Guide needles (leader insertion needles, $1.5\times200$ mm$^2$, Nucletron, Veenendaal, The Netherlands) are then inserted through holes on the insertion plate and into the ones in the exiting plate (indicated in Fig. 1) arranged in a grid template. These holes are parallel on the plates on both sides of the breast. 2DUS is used in conjunction with the template in order to provide trajectory guidance for insertion of the brachytherapy needles.

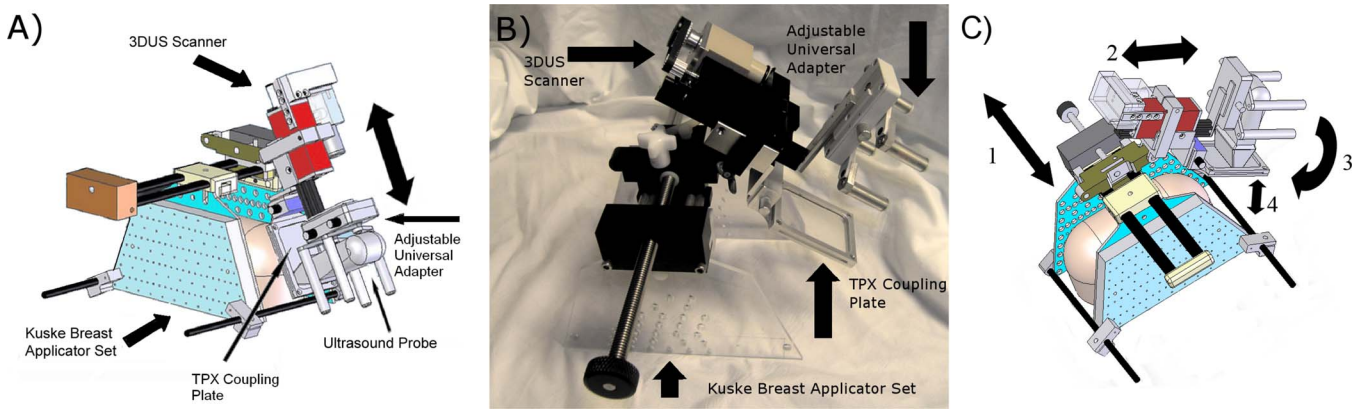


FIG. 2. (a) Schematic illustration of the 3DUS translation scanner mounted on top of the Kuske breast applicator set. Linear scanning motion is indicated by the two-headed arrow. (b) Photograph of 3DUS translation scanning system, with covers removed, mounted on the Kuske breast applicator set. (c) A schematic illustration of the system showing the methods used to adjust the scanning plane to conform to variable breast geometries and sizes and tumor cavity location: (1) A leadscrew is used to adjust the scanner's position along the axis perpendicular to the plane of the compression plates. (2) The scanning plane's position relative to the swivel joint where it is mounted can be adjusted. (3) The scanner is lowered onto the breast, where it is locked in place. The swivel joint enables it to fit onto breasts of different sizes. (4) The TPX plate's position can also be adjusted in order to accommodate different breast sizes.

Initially, three leader insertion needles are inserted through the breast to hold the template in place relative to the breast. The patient is then moved to a CT suite where a preplanning scan is obtained. From this scan, the position of the tumor bed is determined and the tumor margin is added. These data enable the medical physicists to manually determine which catheters are to be implanted for final radiation delivery. The patient is subsequently returned to the brachytherapy suite for the insertion of the remaining guide needles, which are used to guide plastic catheters into the patient.

After all the catheters are implanted, the patient is returned to the CT suite for a final treatment planning scan. Catheter positions relative to the tumor margin, as determined by the scan, are used to plan radiation delivery. Radiation delivery is accomplished by a remote HDR afterloader (Microselectron HDR, Nucletron, Veenendaal, The Netherlands) with a $^{192}$Ir source attached to the catheters. Ten 3.4 Gy radiation treatments are delivered to the breast (total dose=340 Gy) following a protocol of two treatments per day for 5 days with a minimum of 6 h separating each treatment.

## II. MATERIALS AND METHODS

### II.A. 3DUS scanning

Our aim is to replace CT with 3DUS imaging as the principal treatment planning technique without changing any other aspects of the current procedure. In order to achieve this, a 3DUS translation scanner made to fit onto a Kuske breast applicator set was designed and built. The 3DUS translation scanner mechanism is shown attached to the Kuske breast applicator set in Fig. 2. The 3DUS translation scanner can be mounted on the template by a swivel joint on each side of the breast to accommodate variable tumor geometry. Figure 2(c) further displays the degrees of freedom in each direction the user will have to adjust the 3DUS translation scanner in order to accommodate variable breast geometries and sizes. The 3DUS translation scanner is also shown on its own in Fig. 3, where details of individual parts can be seen. The scanner's position along the axis parallel to needle insertion is controlled by a long lead screw mounted above the template. In order to achieve physical coupling, the scanner is lowered to the breast and the swivel joint is tightened, locking the 3DUS translation scanner in a fixed position. US coupling to the breast tissue while maintaining consistent linear geometry was achieved using a coupling plate 7.68 cm long, 6.00 cm wide, and 0.20 cm thick made of TPX plastic.[17] The US probe is held in a vertical position over the coupling plate by an adjustable universal adapter. Both the coupling plate and the scanner's positions are adjustable to accommodate different breast geometries. The TPX plate is coupled to the US probe and the breast tissue through a layer of US gel. A DC motor (1331T 006SR DC micromotor, MicroMo Electronics, Clearwater, FL) is used to drive the lead screw, which controls the linear motion of

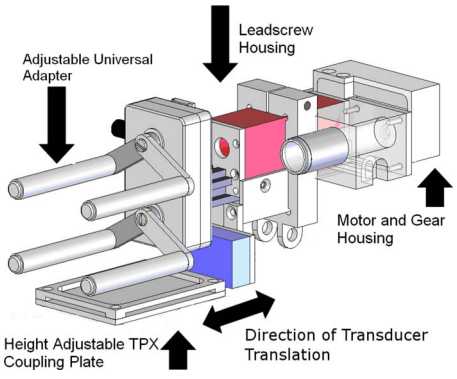


FIG. 3. Schematic illustration of the 3DUS translation scanner on its own. The ultrasound transducer is held by an adjustable universal adapter capable of holding any manufacturer's US transducer. The TPX coupling plate can be adjusted to accommodate different breast sizes. The direction of transducer translation during the scan is indicated.

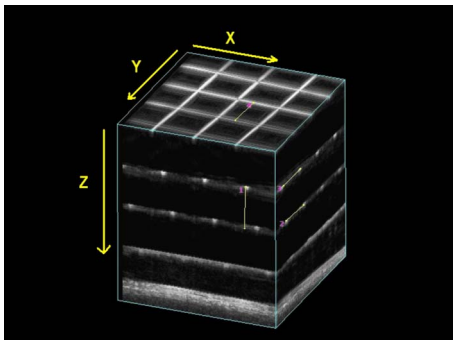


FIG. 4. 3DUS image of a string phantom with measurements marked in each Cartesian direction as indicated.

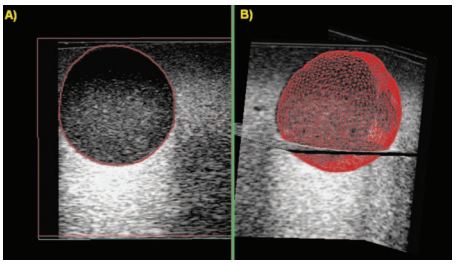


FIG. 5. (a) A 2D cross section and (b) 3D mesh contour of a segmented 25.5 mm diameter spherical simulated "tumor" cavity from a 3DUS image of an agar phantom.

the US probe along the surface of the TPX plate. An encoder (IE2-400, MicroMo Electronics, Clearwater, FL) is integrated into the motor, allowing it to be controlled by a PC, to which it is linked by a serial cable.

All images in our validation studies were acquired using a HDI 3500 (Philips Healthcare, Andover, MA) US imaging system. A 7 MHz broadband linear array transducer (L7-4, Philips Healthcare, Andover, MA) was employed with the system to acquire images. The mechanical 3DUS translation scanner acquires parallel images in the elevational direction. The scanner acquired 200 images over a 50 mm maximum scan length in the elevational direction at a rate of 30 frames/s for a total scanning time of 7.3 s. The US transducer's elevational or out-of-plane resolution is approximately 1.8 mm and is the limiting factor in determining the maximum distance between acquired 2DUS images to avoid aliasing. However, we oversample the elevation direction and acquired 2DUS images separated by a distance of 0.25 mm. Thus, the nominal voxel dimensions used in image reconstruction were set to $0.25 \times 0.24 \times 0.25$ mm$^3$.

## II.B. Experimental procedure

### II.B.1. Linear measurement accuracy

Since the 3DUS images will be used to determine the catheter locations for use in dosimetric calculations, the geometric accuracy of the system needed to be verified. This was achieved by imaging a 3D string phantom, which consists of four layers of fine fishing line separated by $10.00 \pm 0.05$ mm. In each layer, 18 strings are arranged in a grid; 9 run parallel to one another in one direction, and 9 others run in a direction perpendicular to the first set of strings. String separation within each layer is $10.00 \pm 0.05$ mm. Figure 4 shows a 3DUS image of the string phantom. While it was imaged, the phantom was immersed in a 7% glycerol solution, with a speed of sound of 1540 m/s.[18] The scanner was mounted securely above the immersed phantom, with the ultrasound probe's scanning surface submerged just underneath the surface of the solution. 3DUS images were obtained by acquiring 200 2DUS images of the phantom over 40 mm along the $y$ axis indicated in Fig. 4 and reconstructing them into a 3D volume. In each Cartesian direction, we obtained center-to-center distance measurements between five pairs of adjacent strings. The means and standard deviations of each set of measurements were then calculated. A t-test was performed for each direction to determine whether the differences between measured distances and the known values of 10.00 mm were statistically significant.

### II.B.2. Volume measurement accuracy

Determining volumetric measurement accuracy of objects of known volume was necessary to determine whether the system could properly detect the margins of tumor cavities. Phantoms made of agar were used to simulate breast tissue[19] and consisted of simulated postsurgical "tumor" cavities embedded within a background matrix. The background was composed of a solidified mixture of water, agar, glycerol, and sigma cell (concentrations by mass of 86%, 3%, 8%, and 3%, respectively), giving it an acoustic velocity of approximately 1540 m/s, an attenuation coefficient of 6.53 dB/cm at 7 MHz, and a speckle pattern similar to that of breast tissue.[19]

Simulated spherical tumor cavities of known volumes (8.48 and 15.12 cm$^3$) did not contain any scattering agent in order to appear highly hypoechoic in the 3DUS images. Known volume values were obtained by filling the moulds used to construct the simulated tumor cavities with water, then measuring the water's volume with a pipette accurate to 0.1 cm$^3$. Tumor cavities were imaged using the 3DUS translation scanner and then segmented manually along a parallel axis using segmentation software developed in our laboratory.[20,21] The tumor cavity was segmented in a series of parallel 2D slices separated by 1 mm, which were then used to reconstruct a 3D tumor cavity volume. Slices were separated by 1 mm instead of 0.25 mm because the degradation of elevational resolution with increasing depth would provide no advantage to a smaller slice separation value. Figure 5 shows a 2D segmented slice and a 3D surface contour of a 3DUS image of a segmented 25.5 mm diameter spherical simulated tumor cavity. Five volume measurements were obtained from each 3DUS scan of the simulated tumor cavities, and the mean and standard deviation of each volume measurement were then calculated and compared to the known value. A t-test was performed to determine whether the difference between the values measured by segmentation and the known values were statistically significant.

### II.B.3. Image acquisition

In order for the 3DUS images to be sufficient by themselves for treatment planning, it is most important to extract accurate positions of the catheters within the breast tissue. To simulate the final procedure, we constructed an agar phantom with the same composition described previously to simulate the breast tissue. The phantom was placed between the compression plates of an in-house replica of a Kuske breast applicator kit and 16 brachytherapy needles were inserted into the phantom according to a treatment template already used in a procedure at the CHUQ in Quebec City. 200 2DUS images of the phantom were acquired utilizing the 3DUS translation scanner and were subsequently reconstructed into a 3DUS image. Needles were inserted in a specific order: Those in the row farthest from the scanning plane were inserted into the phantom first, followed by those in the next farthest row, and so on. After each row of needles was inserted, a 3DUS image was acquired. It was necessary to follow this specific order for the needle insertion and image acquisition to ensure that no important information about the locations of the more deeply embedded needles was lost due to shadowing from the needles closer to the scanning plane.

### II.B.4. Comparison with CT scan

In order to accurately determine whether 3DUS can effectively replace CT as the primary imaging modality used for treatment planning, we compared 3DUS's ability to localize catheters in breast tissue to CT. An agar phantom with the same composition described previously was used to simulate breast tissue. To allow the registration of 3DUS and CT images, 1.5 mm diameter stainless steel beads were embedded within the agar phantom to act as fiducials.[22]

Within 1 h after completing the 3DUS imaging, the phantom, still compressed between the Kuske breast applicator set and with all catheters still in place, was imaged using a volumetric cone beam micro-CT system (eXplore Locus Ultra, GE Healthcare, London, ON). The scanner was set to 80 kVp and 70 mA. An 8 s anatomical scan was used with 456 projection angles and a slice thickness of 0.9 mm. The in-plane resolution of the micro-CT system is 150 $\mu$m.[23] Each slice measured $1024\times1024$ pixels, and images were composed of 360 parallel slices. Nominal voxel size was set to $0.154\times0.154\times0.154$ mm$^3$.

The CT image was then registered with all of the acquired 3DUS images using point-based rigid-body registration using 1.5 mm embedded stainless steel spheres as fiducials. Figure 6 shows 2D slices of a CT image with all catheters inserted, registered 3DUS image with only a row of the most deeply embedded catheters inserted and registered 3DUS image with all catheters inserted. For 3DUS images with less than five catheters inserted, eight fiducial points were used in order to minimize registration error.[24] However, for 3DUS images with five or more inserted catheters, only six fiducial points were used, as some were obscured by the inserted catheters.

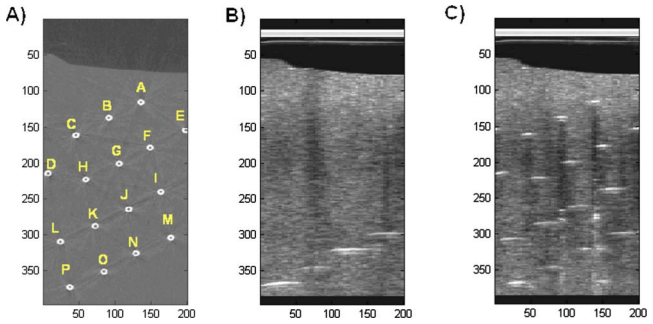


FIG. 6. A 2D cross section of a CT scan of an agar phantom with all catheters inserted (a), a 2D cross section of a 3DUS image of the phantom, acquired in the axial—elevational plane with only the four most deeply embedded catheters inserted (b) and a 2D cross section of 3DUS image of the phantom with all catheters inserted (c). These images are all registered with one another. Catheter "O" in (b) is obstructed slightly by some weak coupling between the TPX plate and the phantom caused by a bubble in the US gel.

### II.B.5. Catheter segmentation

To plot catheter trajectories in both 3DUS and CT images, 15 2D slices separated by an interval of 1.6 mm were used as the data to map trajectories. These 2D slices were composed of eight sequential slices summed together, thereby reducing the effect of noise on the image quality. Semiautomated software was developed in MATLAB to segment the catheters from the surrounding agar in 3DUS images and plot their trajectories. In 2D slices of the 3DUS images, points along the catheter trajectory were detected by finding the point of greatest image intensity in a specific region of interest. This region of interest, which was selected manually on the first slice around the approximate position of the catheter, remains constant on the other 14 slices. In 2D slices of CT images, the first step was again to manually select a region of interest around the approximate catheter location in the first slice. As with the 3DUS images, the region of interest selected on the first 2D slice of the CT image remained constant on the other 14 slices. In both sets of images, it was possible to use a constant region of interest in all the slices because the catheter trajectory's angle with the segmentation plane is small. Unlike with the 3DUS images, however, the point on the catheter's trajectory was located by finding the regional minima of the selected area and then determining the minimum with the lowest overall intensity. The regional minima at the center of the catheter are caused by air at the center of the catheters. Principal component analysis[25] was used to produce a line of best fit through these points, which corresponded to the catheter trajectory.

In order to quantify the 3DUS translation scanner's accuracy in locating catheters, we needed to quantitatively compare the trajectories of catheters segmented from 3DUS images to the trajectories corresponding to the same catheters in CT images. First, angular separation between the trajectories was calculated by using the following formula:

TABLE I. Results of volumetric measurements performed on simulated agar tumor cavities. t-tests were performed and determined no statistical significance in the uncertainties.

| Simulated cavity diameter (mm) | Physical measured volume ($cm^3$) | Segmented measured volume ($cm^3$) | Error ($cm^3$) | Percent error (%) |
|---|---|---|---|---|
| 25.5 | $8.5 \pm 0.1$ | $8.59 \pm 0.10$ | 0.1 | 1.2 |
| 32.0 | $15.1 \pm 0.1$ | $14.84 \pm 0.26$ | 0.3 | 1.87 |

$$\text{Angle} = \arccos\left(\frac{\vec{A} \cdot \vec{B}}{\|\vec{A}\|\|\vec{B}\|}\right), \quad (1)$$

where $A$ and $B$ are the vectors corresponding to the respective catheter trajectories being compared. The maximum and mean distances between the catheter trajectories were also measured to determine the potential differences in dose distributions calculated using 3DUS and CT. The maximum distance between corresponding catheter trajectories is the greatest distance between matched points along each computed trajectory. The mean separation distance is the average distance between these matched points.

## III. RESULTS

### III.A. String phantom imaging

Figure 4 shows a 3DUS image of the string phantom with string measurements acquired in three Cartesian directions. In Fig. 4, the $y$ axis signifies the elevational direction (the direction of the 3DUS scan), the $x$ axis denotes the lateral direction of the US images, and the $z$ axis represents the axial direction. String separation was measured to be $1.00 \pm 0.01$ cm in the $x$ direction, $1.01 \pm 0.01$ cm in the $y$ direction, and $1.01 \pm 0.02$ cm in the $z$ direction. Mean measurements agreed within 1% uncertainty to the nominal value of 1 cm. A t-test ($\alpha=0.05$, $1-\beta=0.8$, and $p=0.24, 0.56, 0.29$) showed no statistically significant difference between known and measured values of string separations in each of the coordinate axis.

TABLE II. Summary of the results obtained comparing corresponding catheter trajectories segmented from CT and 3DUS images.

| Catheter | Angular trajectory separation (deg) | Maximum trajectory separation (mm) | Mean trajectory separation (mm) |
|---|---|---|---|
| A | 2.1 | 0.92 | 0.51 |
| B | 0.77 | 0.16 | 0.15 |
| C | 2.78 | 0.82 | 0.54 |
| D | 0.7 | 0.29 | 0.15 |
| E | 0.93 | 1.59 | 1.33 |
| F | 1.19 | 0.93 | 0.59 |
| G | 2.39 | 0.99 | 0.51 |
| H | 1.36 | 0.35 | 0.26 |
| I | 4.02 | 1.48 | 0.84 |
| J | 4.8 | 1.11 | 0.87 |
| K | 2.72 | 1.85 | 1.45 |
| L | 2.51 | 1.46 | 0.8 |
| M | 1.89 | 1.1 | 0.49 |
| N | 4.11 | 1.15 | 0.83 |
| O | 1.59 | 0.89 | 0.83 |
| P | 3.95 | 1.5 | 0.84 |
| Mean | 2.36 | 1.04 | 0.69 |
| Maximum | 4.8 | 1.85 | 1.45 |

### III.B. Embedded agar sphere imaging

Figure 5 shows a 2D segmented slice and 3D surface contour of 3DUS image of a segmented spherical simulated tumor cavity. Volume accuracy and variability measurements are shown in Table I. Segmented measured volumes agreed within 2% uncertainty to the known spherical volume for each of the simulated agar tumors. t-tests ($\alpha=0.05$, $1-\beta=0.8$, and $p=0.91, 0.32$) failed to show any statistical significance in the differences between measured and known values.

### III.C. Comparison with CT scan for catheter detection

Figure 7 shows a 3D plot of five catheter paths segmented in CT and 3DUS images. Table II shows the results of angular separation, maximum separation distance, and mean separation distance of trajectories of the 16 catheters between the

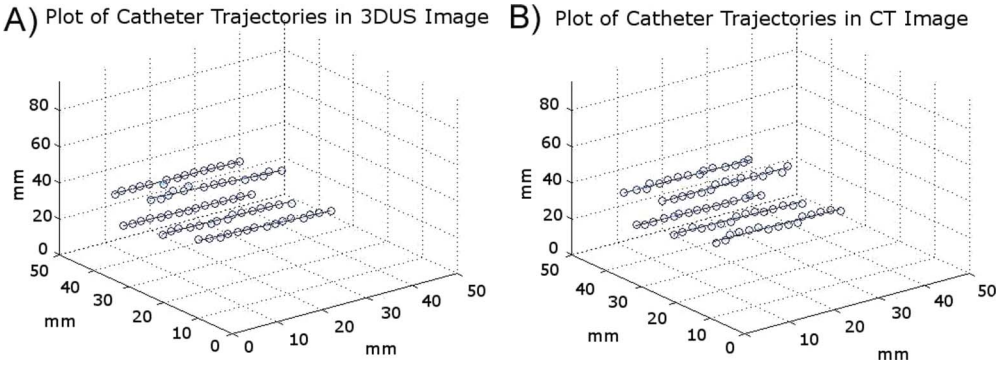


FIG. 7. Segmented needle trajectories shown in 3D space for the 3DUS image (a) and CT image (b).

3DUS and CT images. The average maximum angular separation between catheter trajectories was 2.4°. The average maximum separation distance was 1.0 mm, while the average mean separation distance was 0.7 mm.

## IV. DISCUSSION

Agreement between known and measured volumes for linear and volumetric measurements was within 1% and 2%, respectively. t-tests indicated no statistical significant difference in either measurement. This indicates that the 3DUS translation scanning system is capable of effectively measuring linear dimensions and volumes. It also shows that the system is capable of segmenting tumor margins during the preplanning process.

Since the objective of our experiments was to establish the accuracy of our 3DUS translation scanning system, we used a phantom with the same velocity of sound as is used in the ultrasound machine to avoid geometrical distortions. The 7% glycerol solution and agar phantoms used in this study assumed an acoustic velocity of 1540 m/s even though studies have shown breast tissue to have variable composition of adipose and glandular tissue, and thus, a variable acoustic velocity between 1450 and 1560 m/s.[26–28] Compensating for geometrical distortion caused by mismatch between the velocity of sound assumed by the ultrasound machine and the velocity of sound of the various tissues in the breast will require the development of a technique to segment and classify the tissues in the 3DUS images and then correct the geometry based on the estimated speed of sound for those tissues

Only two of the segmented needles showed a maximum trajectory distance between imaging modalities of greater than 1.5 mm, the diameter of the segmented catheters. None of the mean separation distances between catheter trajectories in 3DUS and CT were greater than 1.5 mm. The maximum trajectory distance between any of the corresponding catheters was 1.85 mm, which is not significant compared to the mean free path of $\gamma$-rays produced by $^{192}$Ir in water (100 mm). This indicates a minimal effect on the final dose distribution if the same dose plan were performed using either 3DUS or CT. Further research beyond the scope of this study would be required to confirm this. The mean angular separation distance between catheter trajectories segmented from 3DUS and CT images was 2.4°. These results showcase the 3DUS translation scanner's ability to accurately locate catheter trajectories in breast tissue. These findings suggest the 3DUS translation scanning system could potentially be integrated into the brachytherapy suite and be used as a treatment planning device on cancer patients.

A maximum angular separation distance of 4.8° indicates the segmentation algorithm should be enhanced in an effort to improve the scanner's segmentation of catheter direction. It will also be necessary to automatically register the catheter's locations with the grid on the brachytherapy template in near-real time as the catheters are being inserted to facilitate integration with the treatment planning system.

## V. CONCLUSIONS

The 3DUS translation scanning system's ability to accurately image and measure the volumes of simulated agar tumor cavities show its ability to accurately measure volumes of known objects. This indicates its potential to accurately image and segment tumor cavities following surgical lumpectomy, which appear highly hypoechoic in US images. This, as well as the 3DUS translation scanner's ability to produce images in near-real time, showcases the system's potential as a preplanning tool to determine which catheters to insert in breast brachytherapy.

The system's ability to produce images in the brachytherapy suite eliminates the need to move the patient back and forth from the CT suite. This reduces the time and manpower needed to perform the procedure, thus reducing the final cost as well. It also negates the potential for the tumor cavity geometry relative to the brachytherapy template to change while the patient is being moved after the preplanning scan.

The system was also capable of accurately locating catheters inserted into an agar breast phantom. Segmented catheter trajectories using the 3DUS translation scanning system were very close to those segmented from CT images, the current imaging standard for treatment planning in breast brachytherapy. The 3DUS translation scanning system's ability to track the catheter positions as they are being inserted present an additional advantage over the CT system. As well, as catheters are being inserted, the 3DUS translation scanning system enables the user to view any geometrical distortion to the tumor cavity that might occur. This allows them to adjust which catheters to insert into the breast to best suit the modified tumor cavity geometry. We will soon be testing the 3DUS translation scanning system clinically at the Centre Hospitalier Universitaire de Québec (CHUQ).

## ACKNOWLEDGMENTS

The authors would like to thank Jeff Bax and Jacques Montreuil for their help with the mechanical design and construction of the scanner, Lori Gardi for her software design and development, Mike Bygrave for his assistance in using the micro-CT scanner, and Annie Letourneau and Dr. Anne Dagnault for their advice and for providing the clinical implant pattern. The authors acknowledge the following sources of funding: The Canadian Breast Cancer Research Alliance and the Canadian Institutes of Health Research. The last author (A.F.) holds a Canada Research Chair in Biomedical Engineering, and acknowledges the support of the Canada Research Chair program. P.D. acknowledges the support of the Canadian Institutes of Health Research Strategic Training Program in Cancer Research and Technology Transfer.

[a]Electronic mail: pdejean@imaging.robarts.ca

[1]B. Fisher, S. Anderson, J. Bryant, R. G. Margolese, M. Deutsch, E. R. Fisher, J. H. Jeong, and N. Wolmark, "Twenty-year follow-up of a randomized trial comparing total mastectomy, lumpectomy, and lumpectomy plus irradiation for the treatment of invasive breast cancer," N. Engl. J. Med. **347**(16), 1233–1241 (2007).

[2]U. Veronesi *et al.*, "Breast conservation is the treatment of choice in small breast cancer: Long-term results of a randomized trial," Eur. J. Cancer **26**(6), 668–670 (1990).
[3]K. L. Baglan, A. A. Martinez, R. C. Frazier, V. R. Kini, L. L. Kestin, P. Y. Chen, G. Edmundson, E. Mele, D. Jaffray, and F. A. Vicini, "The use of high-dose-rate brachytherapy alone after lumpectomy in patients with early-stage breast cancer treated with breast-conserving therapy," Int. J. Radiat. Oncol., Biol., Phys. **50**(4), 1003–1011 (2001).
[4]D. W. Arthur, D. Koo, R. D. Zwicker, S. Tong, H. D. Bear, B. J. Kaplan, B. D. Kavanagh, L. A. Warwicke, D. Holdford, C. Amir, K. J. Archer, and R. K. Schmidt-Ullrich, "Partial breast brachytherapy after lumpectomy: Low-dose-rate and high-dose-rate experience," Int. J. Radiat. Oncol., Biol., Phys. **56**(3), 681–689 (2003).
[5]B. Fisher and S. Anderson, "Conservative surgery for the management of invasive and noninvasive carcinoma of the breast: NSABP trials. National surgical adjuvant breast and bowel project," World J. Surg. **18**(1), 63–69 (1994).
[6]K. Holli, R. Saaristo, J. Isola, H. Joensuu, and M. Hakama, "Lumpectomy with or without postoperative radiotherapy for breast cancer with favourable prognostic features: Results of a randomized study," Br. J. Cancer **84**(2), 164–169 (2001).
[7]O. J. Ott, G. Hildebrandt, R. Potter, J. Hammer, M. Lotter, A. Resch, R. Sauer, and V. Strnad, "Accelerated partial breast irradiation with multicatheter brachytherapy: Local control, side effects and cosmetic outcome for 274 patients. Results of the German Austrian multi-centre trial," Radiother. Oncol. **82**(3), 281–286 (2007).
[8]G. Jozsef, G. Luxton, and S. C. Formenti, "Application of radiosurgery principles to a target in the breast: A dosimetric study," Med. Phys. **27**(5), 1005–1010 (2000).
[9]S. C. Formenti, "External-beam-based partial breast irradiation," Nat. Clin. Pract. Oncol. **4**(6), 326–327 (2007).
[10]M. Keisch, F. Vicini, R. R. Kuske, M. Hebert, J. White, C. Quiet, D. Arthur, T. Scroggins, and O. Streeter, "Initial clinical experience with the MammoSite breast brachytherapy applicator in women with early-stage breast cancer treated with breast-conserving therapy," Int. J. Radiat. Oncol., Biol., Phys. **55**(2), 289–293 (2003).
[11]D. H. Clarke, F. A. Vicini, and H. Jacobs, "High dose rate brachytherapy for beast cancer," *High Dose Rate Brachytherapy—A Textbook*, edited by S. Nag (Futura Publishing, Arnonk, NY, 1994), pp. 321–329.
[12]R. R. Kuske *et al.*, "Brachytherapy as the sole method of breast irradiation in TIS, T1, T2, No-1 breast cancer (Abstract)," Int. J. Radiat. Oncol., Biol., Phys. **30**(1), 245 (1994).
[13]F. Perera, F. Chisela, J. Engel, and V. Venkatesan, "Method of localization and implantation of the lumpectomy site for high dose rate brachytherapy after conservative surgery for T1 and T2 breast cancer," Int. J. Radiat. Oncol., Biol., Phys. **31**(4), 959–965 (1995).
[14]F. Perera, J. Engel, R. Holliday, L. Scott, M. Girotti, D. Girvan, F. Chisela, and V. Venkatesan, "Local resection and brachytherapy confined to the lumpectomy site for early breast cancer: A pilot study," J. Surg. Oncol. **65**(4), 263–267 (1997).
[15]P. R. Benitez, P. Y. Chen, F. A. Vicini, M. Wallace, L. Kestin, G. Edmundson, G. Gustafson, and A. Martinez, "Partial breast irradiation in breast conserving therapy by way of intersitial brachytherapy," Am. J. Surg. **188**(4), 355–364 (2004).
[16]T. A. King, J. S. Bolton, R. R. Kuske, G. M. Fuhrman, T. G. Scroggins, and X. Z. Jiang, "Long-term results of wide-field brachytherapy as the sole method of radiation therapy after segmental mastectomy for T(is,1,2) breast cancer," Am. J. Surg. **180**(4), 299–304 (2000).
[17]R. C. Booi, J. F. Krucker, M. M. Goodsitt, M. O'Donnell, A. Kapur, G. L. LeCarpentier, M. A. Roubidoux, J. B. Fowlkes, and P. L. Carson, "Evaluating thin compression paddles for mammographically compatible ultrasound," Ultrasound Med. Biol. **33**(3), 472–482 (2007).
[18]S. Tong, D. B. Downey, H. N. Cardinal, and A. Fenster, "A three-dimensional ultrasound prostate imaging system," Ultrasound Med. Biol. **22**(6), 735–746 (1996).
[19]D. W. Rickey, P. A. Picot, D. A. Christopher, and A. Fenster, "A wall-less vessel phantom for Doppler ultrasound studies," Ultrasound Med. Biol. **21**(9), 1163–1176 (1995).
[20]H. M. Ladak, F. Mao, Y. Wang, D. B. Downey, D. A. Steinman, and A. Fenster, "Prostate boundary segmentation from 2D ultrasound images," Med. Phys. **27**(8), 1777–1788 (2000).
[21]Y. Wang, H. N. Cardinal, D. B. Downey, and A. Fenster, "Semiautomatic three-dimensional segmentation of the prostate using two-dimensional ultrasound images," Med. Phys. **30**(5), 887–897 (2003).
[22]C. R. Maurer, G. B. Aboutanos, B. M. Dawant, R. J. Maciunas, and J. M. Fitzpatrick, "Registration of 3-D images using weighted geometrical features," IEEE Trans. Med. Imaging **15**(6), 836–849 (1996).
[23]L. Y. Du, J. Umoh, H. N. Nikolov, S. I. Pollmann, T. Y. Lee, and D. W. Holdsworth, "A quality assurance phantom for the performance evaluation of volumetric micro-CT systems," Phys. Med. Biol. **52**(23), 7087–7108 (2007).
[24]J. M. Fitzpatrick, J. B. West, and C. R. Maurer, Jr., "Predicting error in rigid-body point-based registration," IEEE Trans. Med. Imaging **17**(5), 694–702 (1998).
[25]S. Wold, "Principal component analysis," Chemom. Intell. Lab. Syst. **2**(1–3), 37–52 (1987).
[26]D. Pfeiffer, S. Sutlief, W. Feng, H. M. Pierce, and J. Kofler, "AAPM Task Group 128: Quality assurance tests for prostate brachytherapy ultrasound systems," Med. Phys. **35**(12), 5471–5489 (2008).
[27]E. L. Madsen, W. A. Berg, E. B. Mendelson, and G. R. Frank, "Anthropomorphic breast phantoms for qualification of Investigators for ACRIN Protocol 6666," Radiology **239**(3), 869–874 (2006).
[28]W. Weiwad, A. Heinig, L. Goetz, H. Hartmann, D. Lampe, J. Buchmann, R. Millner, R. P. Spielmann, and S. H. Heywang-Koebrunner, "Direct measurement of sound velocity in various specimens of breast tissue," Invest. Radiol. **35**(12), 721–726 (2000).